One-Electron NO to N_2O Pathways via Heme Models and Lewis Acid: Metal Effects and Differences from the Enzymatic Reaction

Jia-Min Chu,[a] Rahul L. Khade,[a] Vy Nguyen,[a] George B. Richter-Addo,[b] and Yong Zhang*[a]

[a] Dr. J.-M. Chu, Dr. R. L. Khade, V. Nguyen, Prof. Dr. Y. Zhang
Department of Chemistry and Chemical Biology
Stevens Institute of Technology
1 Castle Point Terrace, Hoboken, NJ 07030, United States
E-mail: yong.zhang@stevens.edu

[b] Dr. G. B. Richter-Addo
Department of Chemistry and Biochemistry
University of Oklahoma, Norman, OK 73019, United States

Supporting information for this article is given via a link at the end of the document.

Abstract: Some pathogens use heme-containing nitric oxide reductases (NORs) to reduce NO to N_2O as their defense mechanism to detoxify NO and reduce nitrosative stress. This reduction is also significant in the global N cycle. Our previous experimental work showed that Fe and Co porphyrin NO complexes can couple with external NO to form N_2O when activated by the Lewis acid BF_3. A key difference from conventional two-electron enzymatic reaction is that one electron is sufficient. However, a complete understanding of the entire reaction pathways and the more favorable reactivity for Fe remains unknown. Here, we present a quantum chemical study to provide such information. Our results confirmed Fe's higher experimental reactivity, showing advantages in all steps of the reaction pathway: easier metal oxidation for NO reduction and N-O cleavage as well as a larger size to expedite the N/O coordination mode transition. The Co system, with a similar product energy as the enzyme, shows potential for further development in catalytic NO coupling. This work also offers the first evidence that this new one-electron NO reduction is both kinetically competitive and thermodynamically more favorable than the native pathway, supporting future initiatives in optimizing NO reduction agents in biology, environment, and industry.

Introduction

Nitric oxide (NO) is involved in signaling as part of cardiovascular regulation, in the immune response, neurotransmission, and other physiological processes.[1] As a signaling molecule, its concentration needs to be properly maintained. However, high concentration of NO are employed by some organisms such as macrophages to elicit cytotoxic activity against viruses, bacteria, fungi, protozoa, helminths, and tumor cells.[2] Nevertheless, some pathogens have evolved the defense mechanism using nitric oxide reductases (NORs) to mitigate the nitrosative stress.[3] Bacterial NORs (bacNORs) are well-known for their significant roles in the global N-cycle that is of broad general biological, environmental, and industrial importance.[1b, 3a, b, 4]

bacNORs utilize a di-Fe heme b_3:non-heme Fe_B site to couple two NO molecules to generate N_2O.[5] Among three proposed bacNOR mechanisms (*cis*:b_3, *trans*, and *cis*:Fe_B, see Scheme 1A),[5b, 6] two of them involve the ferrous (por)Fe(NO) (por = porphyrin) fragment to react with external NO. However, (por)Fe(NO) compounds in isolation are unreactive towards external NO for N_2O generation.[6h, 7] Interestingly, our previous experimental work demonstrated that a synthetic monoheme-NO model activated by Lewis acids (LAs) was susceptible to attack by external NO for N–N bond coupling toward N_2O formation, which were supported by IR and X-ray crystallography studies and computational results.[8]

This activation highlights the important role that Lewis acids play in enabling novel reactions or improving reactivity of existing reactions as reported previously. For instance, Goldberg's work demonstrated extensively the use of Lewis acids to modulate the reactivity of metal-oxo species.[9] Similarly, Nam and Fukuzumi's studies showed that Lewis acids can enhance reactivity of metal-oxygen intermediates in redox reactions and significantly improve the photocatalytic reactivity of organic photocatalysts by increasing their redox potential.[10] Earlier studies by Doyle revealed that Lewis acids like BF_3 can activate diazo compounds, enabling highly efficient carbene transfer reactions that are useful in organic synthesis.[11] Numerous other studies have also demonstrated the diverse applications of Lewis acids to enhance electrophilicity, stabilize reactive intermediates, and improve selectivity in catalytic reactions.[12]

Our calculations of reactants and N-N coupled intermediates provided useful geometric and electronic data to understand the unreactive origin of (por)Fe(NO) with external NO alone and the key roles of a LA to effect this new reaction via a previously unknown synergistic effect with heme, which is reminiscent of the native bacNOR with both a heme center and a nearby non-heme site as a potential LA. Results demonstrated that the Lewis acid BF_3 induces 1) a large negative charge on proximal NO by facilitating charge transfers from either the metal center in Fe porphyrin or the porphyrin in Co porphyrin, and 2) correspondingly positive charge on distal NO, to enhance electrostatic attraction between these two oppositely charged NO molecules toward the N–N coupling.[8, 13] Significant changes were also found with the NO and/or ONNO bound complexes' structures as well as NO coupling energies upon the addition of BF_3.

A key difference from the conventional NOR mechanisms with a two-electron reduction process is that one electron is sufficient for this new NO-to-N_2O conversion. There is a growing interest in exploring the feasibility of one-electron pathway with heme/non-

heme binuclear sites and nonheme NOR complexes in order to understand their reaction mechanisms.[3c, 14]

However, for this novel one-electron NO-to-N_2O pathways of heme systems, except for our previous calculations of the N-N coupled intermediates, reactants, and by-products for Fe and Co hemes,[8, 13] the mechanistic results of the complete reaction pathways of each step toward final product, the rate-determining step (RDS), and especially the overall kinetic and thermodynamic features, are still unknown. In addition, Co heme reacts slower than Fe and these two systems exhibit porphyrin and metal oxidation respectively in the one-electron NO reduction pathways.[8, 13] This significant differential metal center effect on this novel one-electron NO-to-N_2O pathways of heme systems has not been elucidated yet. Metals were found to affect mechanisms and reactivities in both heme catalyzed non-native carbene transfer reactions[15] and native transformations by heme copper oxidases (HCOs)[6i, 16] which are evolutionarily, structurally and functionally related to NORs. The non-heme metal centers were also found in a recent work to influence HCO's NO reduction mechanism.[17] However, there has been no comparative mechanistic study of the new one-electron reaction vs. the known two-electron process in native bacNORs.

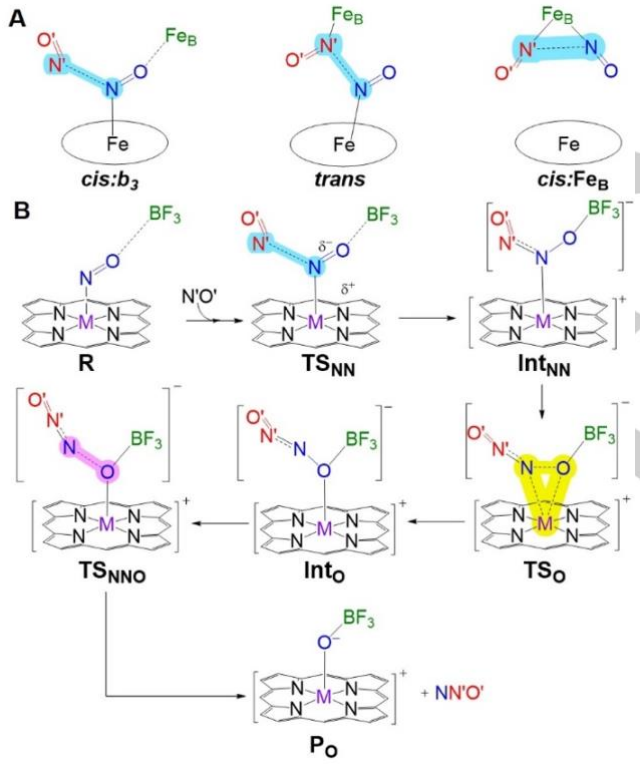

Scheme 1. (A) Three proposed mechanisms for NO coupling by bacNOR. Oval represents heme. **(B)** Proposed pathway for the complete one-electron NO to N_2O reduction via heme activated by BF_3. M = Fe or Co. Key atoms involved in transition states are color coded as follows: blue for N–N bond formation, yellow for metal binding mode transition, and pink for NO cleavage.

To provide these missing mechanistic results, a quantum chemical investigation using the method which accurately revealed reactivities of similar NO-containing heme systems[8, 13, 18] was conducted for the proposed one-electron pathway shown in Scheme 1 for both Fe and Co porphyrins, the currently only known experimental model systems for this novel NO coupling mechanism.[8, 13] It starts with the attack of an external NO (labeled as N'O') to the heme-nitrosyl complex **R** to form the metal bound hyponitrite intermediate $\mathbf{Int_{NN}}$ through the N–N coupling (see blue highlight in Scheme 1) transition state $\mathbf{TS_{NN}}$. Then the hyponitrite intermediate undergoes a binding mode transition ($\mathbf{TS_O}$) with yellow highlight to generate the O-coordinated $\mathbf{Int_O}$. In the last step, the N–O bond (in salmon highlight, Scheme 1) breaks via $\mathbf{TS_{NNO}}$, resulting in N_2O cleavage to form the final product $\mathbf{P_O}$, which can be readily protonated to form the experimentally characterized neutral product complex.[8, 13] This overall pathway resembles the steps in the previously reported most favorable two-electron *cis:b3* mechanism of the native NOR reaction,[6c, d] since both types of reactions contain a common heme site and a distal non-heme site acting as a LA. However, our results of the novel Fe/Co one-electron pathways show significant geometric, kinetic, and thermodynamic feature differences from the two-electron process (*vide infra*), which also reproduced the experimentally observed more reactive nature for the Fe-heme model compared to Co.[8, 13]

Results and Discussion

As shown in Scheme 1, the first step is the NO coupling. In the conventional two-electron pathway, the most stable hyponitrite intermediate $\mathbf{Int_{NN}\text{-}Fe_{b3}}$ (the metal center in the heme was added to label of a reaction species to represent that for the specific heme system; Fe_{b3} is the Fe center in heme *b3* site in bacNOR) involves a five-membered ring where both oxygen atoms of the hyponitrite moiety coordinate to the nonheme iron Fe_B as a LA (Figure 1).[6c, d] This transition state $\mathbf{TS_{NN}\text{-}Fe_{b3}}$ is kinetically accessible with a modest Gibbs free energy of activation ($\Delta G^{\ddagger}$), 11 kcal/mol and the formed $\mathbf{Int_{NN}\text{-}Fe_{b3}}$ is thermodynamically favorable with a relative energy from the reactants of -10.1 kcal/mol. In this intermediate, both heme and non-heme iron are oxidized to be Fe^{III} while the hyponitrite moiety is a dianion.

In contrast, the one-electron pathway introduces a novel structural change, where only the oxygen of the heme bound NO bonding to the Lewis acid BF_3, leaving the other oxygen from the external NO non-bonded in $\mathbf{Int_{NN}\text{-}Fe}$, see Figure 1. The formation of the ring structure in $\mathbf{Int_{NN}\text{-}Fe_{b3}}$ has a strong stabilization effect to make it thermodynamically favorable with a relative energy from the reactants of -10.1 kcal/mol. In fact, this ring structure in the so-called *cis:b3* pathway is much more favorable that corresponding NO coupled intermediates with non-ring structures in the other two mechanisms (*trans*, and *cis:*Fe_B, see Scheme 1A) by 35.4 and 24.2 kcal/mol.[17b] Therefore, it is understandable that $\mathbf{Int_{NN}\text{-}Fe}$ without a ring structure is of relatively higher energy in the reaction pathway compared to $\mathbf{Int_{NN}\text{-}Fe_{b3}}$, as seen from Figure 1.

However, the strong O···BF_3 interaction (1.676 Å, Table 1) in the Fe heme model reactant **R-Fe** was found to effect the electron transfer from Fe^{II} to NO to result in oxidized heme Fe,[8] unlike the maintained Fe^{II} in this stage of the native NOR reaction.[6c, d] This strong interaction also facilitates the N−N coupling by inducing the positive distal N'O' (0.133 e) and the negative proximal NO (-0.389 e) for favorable Coulombic attraction in $\mathbf{TS_{NN}\text{-}Fe}$, which leads to a kinetically feasible $\Delta G^{\ddagger}$ of 11.44 kcal/mol. This is close that for the native two-electron process, see Figure 1.

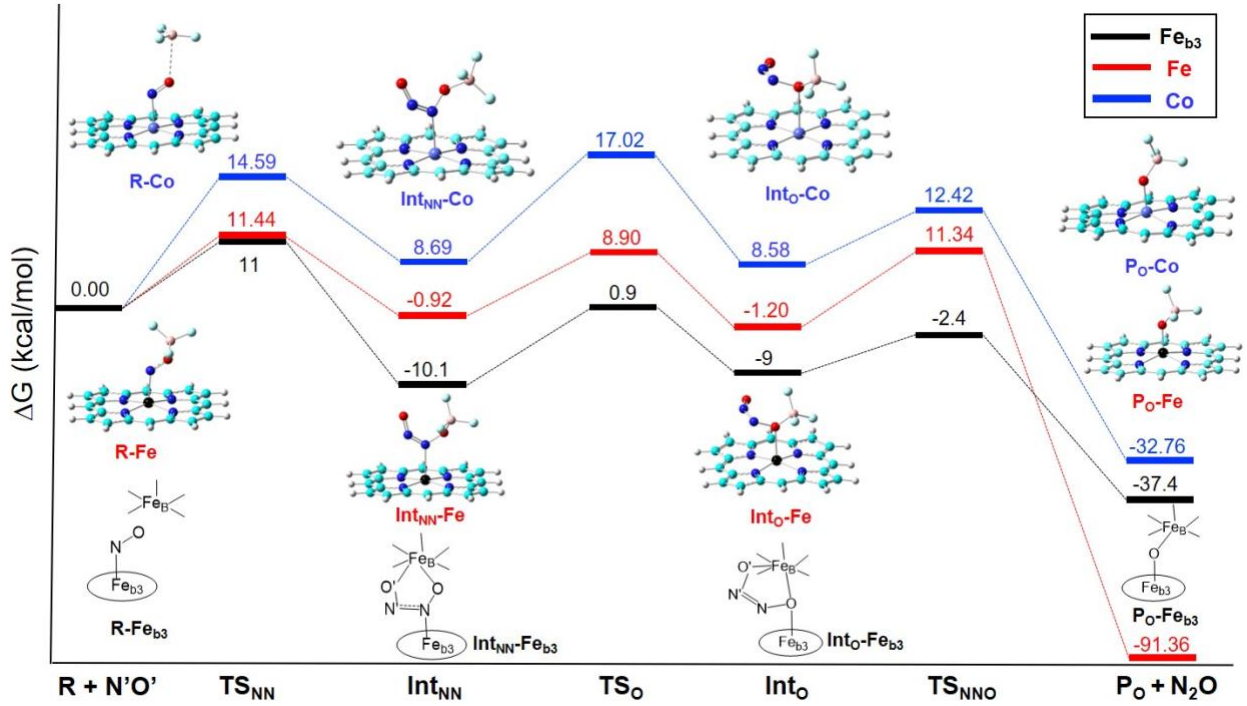

Figure 1. Schematic Gibbs free energy diagram for the one-electron and two-electron NO to N_2O conversion pathways. The optimized structures of all species except for transition states in the one-electron pathways for Fe/Co are shown. The black scheme is the two-electron *cis:b3* mechanism, oval represents the heme with an His axial ligand.[6c, d] Atom color scheme: Fe- black, Co-navy blue, C-cyan, N-blue, O- red, B- pink, F- light blue, H-grey.

Table 1. Key Geometric Parameters, Spin Densities, and Relative Energies of Species Involved in the One-Electron NO to N_2O Conversion

Species	$R_{MN(Por)}$ (Å)	R_{MN} (Å)	R_{MO} (Å)	R_{NO} (Å)	$R_{NN'}$ (Å)	R_{OB} (Å)	$\rho_{\alpha\beta}^{M}$ (e)	$\rho_{\alpha\beta}^{NO}$ (e)	$\rho_{\alpha\beta}^{N'O'}$ (e)	$\rho_{\alpha\beta}^{Por}$ (e)	ΔE (kcal/mol)	ΔE_{zpe} (kcal/mol)	ΔH (kcal/mol)	ΔG (kcal/mol)
R-Fe (+N'O')	1.998	1.910	2.813	1.225	/	1.676	2.657	-1.495	/	-0.140	0.00	0.00	0.00	0.00
TS$_{NN}$-Fe	1.995	1.993	2.892	1.244	2.170	1.610	2.770	-1.307	0.695	-0.126	0.57	1.59	0.92	11.44
Int$_{NN}$-Fe	1.988	2.214	3.206	1.359	1.241	1.513	2.989	0.092	0.987	-0.072	-14.42	-11.34	-12.41	-0.92
TS$_O$-Fe	1.986	2.487	2.496	1.378	1.226	1.532	3.043	0.109	0.967	-0.125	-3.94	-1.56	-2.80	8.90
Int$_O$-Fe	1.989	2.994	2.168	1.423	1.223	1.542	3.030	0.054	1.015	-0.105	-14.78	-11.91	-12.96	-1.20
TS$_{NNO}$-Fe	1.990	3.104	2.135	1.663	1.167	1.506	3.116	0.338	0.703	-0.174	-0.42	1.04	0.08	11.34
P$_O$-Fe (+N_2O)	2.103	/	1.758	/	/	1.438	4.210	0.406[a]	/	-0.642	-94.28	-95.12	-95.44	-91.36
R-Co (+N'O')	1.992	1.946	2.734	1.151	/	2.726	0.876	-0.802	/	-0.067	0.00	0.00	0.00	0.00
TS$_{NN}$-Co	1.999	2.040	2.915	1.295	1.315	1.574	0.947	0.591	0.404	-0.949	0.75	0.96	-0.80	14.59
Int$_{NN}$-Co	2.072	2.162	3.195	1.362	1.240	1.508	2.764	0.024	1.004	-0.793	-3.56	-3.33	-4.53	8.69
TS$_O$-Co	2.074	2.467	2.462	1.381	1.225	1.525	2.762	0.064	0.982	-0.816	5.44	4.98	3.55	17.02
Int$_O$-Co	2.074	2.980	2.140	1.420	1.221	1.532	2.771	0.021	1.004	-0.803	-3.75	-3.76	-4.93	8.58
TS$_{NNO}$-Co	2.079	3.036	2.021	1.653	1.170	1.510	2.778	0.266	0.718	-0.781	0.80	-0.21	-1.43	12.42
P$_O$-Co (+N_2O)	2.088	/	1.725	/	/	1.459	2.991	0.554[a]	/	-0.573	-38.12	-39.04	-40.00	-32.76

[a] spin density of O only.

The Co porphyrin system has a different reaction behavior. In **R-Co**, the O···BF_3 interaction is much weaker as evidenced by a much longer O…B distance of 2.726 Å (Table 1). Probably because oxidizing Co^{II} to Co^{III} is more challenging compared to Fe due to its relatively higher standard reduction potential (E°=1.92V for Co and 0.77 V for Fe),[19] the Co^{II} electronic structure remains throughout the reaction pathway as evidenced by the approximately odd numbers of unpaired electrons illustrated by Co spin densities ($\rho_{\alpha\beta}^{M}$, see Table 1), showing a distinct reaction feature compared to the Fe system. As such, the oxidation occurs in porphyrin upon external NO attack to transfer its electron to proximal NO, forming π-radical cation ($\rho_{\alpha\beta}^{Por}$: -0.949 e in **TS$_{NN}$-Co**, see Table 1). Consistent with the porphyrin oxidation feature, the charge of porphyrin is also significantly increased from **R-Co** to **TS$_{NN}$-Co** by +0.753 e, see Figure 2. **TS$_{NN}$-Co** has a significantly higher barrier of 14.59 kcal/mol than **TS$_{NN}$-Fe**. This shows the reactivity difference between the metal-centered oxidation and the porphyrin ring oxidation.[20]

More detailed geometric and electronic data analysis also support the more reactive N-N coupling with the Fe heme in this novel one-electron pathway. As seen from Figure 2, the N−N bond in **TS$_{NN}$-Fe** is significantly longer than that in **TS$_{NN}$-Co** (2.170 Å and 1.315 Å respectively), indicating an earlier transition state in the Fe system. The significant decrease in the O–B bond (-1.152 Å for Co vs. -0.066 Å for Fe) from **R** to **TS$_{NN}$** also suggests the later transition state feature with a higher energy barrier for Co. Consistent with such relatively earlier and later **TS$_{NN}$** for Fe and Co respectively, the amounts of atomic charge changes and corresponding charge transfers in the Fe system are much smaller than those for Co, as shown in Figure 2. In addition, the higher spin densities of both proximal and distal NOs in **TS$_{NN}$-Fe** present more pronounced radical feature (-1.307 e and 0.695 e respectively in Table 1) compared to the NOs in **TS$_{NN}$-Co** (0.591 e and 0.404 e respectively), indicating favorable radical coupling in the Fe system.

The second step (see Scheme 1B) involves a binding mode transition from N-coordination in **Int$_{NN}$** to O-coordination in **Int$_O$**. As seen from Figure 1, this step is easy in the native two-electron

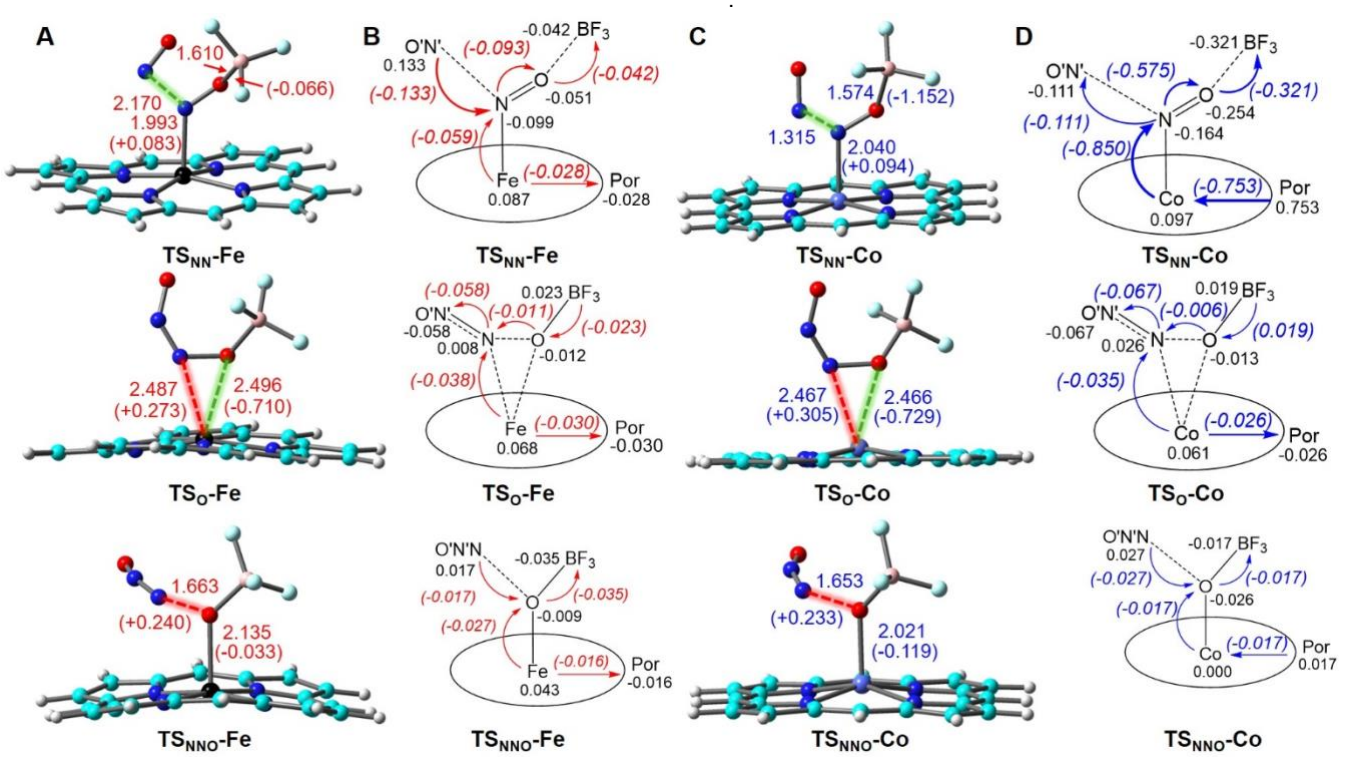

Figure 2. (A,C) Key geometric parameters at transition state and changes from previous species in parentheses (in Å). **(B, D)** key atomic charge changes (in black) and charge transfers by arrows and numbers in parentheses (in e). Numbers in red and blue represent Fe and Co systems respectively. Green dashes highlight bond formation and red dashes highlight bond breakage.

pathway since **TS$_O$-Fe$_{b3}$** has an energy of 0.9 kcal/mol from the starting reactants. The ring structure is maintained when the O-coordinated **Int$_O$-Fe$_{b3}$** is generated.[6c, d] The two intermediates **Int$_{NN}$-Fe$_{b3}$** and **Int$_O$-Fe$_{b3}$** with respectively N or O coordination are of similar energies.

In contrast, while such two intermediates for the one-electron pathways for Fe and Co are still of similar energies (see Figure 1), their transition states are of much higher energies by ~8 and ~16 kcal/mol, respectively, compared to the two-electron pathway. This perhaps is a result of lacking the ring structure in the two-electron process to stabilize the reaction systems. The Fe heme model is of lower barrier than Co, since both the Fe−N and Fe−O bonds in **TS$_O$-Fe** are ~0.03 Å longer than the Co−N and Co−O bonds in **TS$_O$-Co** (see Figure 2) to offer more geometric flexibility and thus lower the energy cost of breaking the original M-N bond to facilitate the binding mode transition. The larger Fe-N/O bond lengths probably come from a larger atomic radius of Fe than Co. As this step involves only coordination mode switch, the changes in atomic charges are smaller compared to the first step of NO coupling, see Figure 2. In both cases, as the binding is shifted from N to the more electronegative O, additional charges (~0.04 e) are transferred from the metal center to this NO moiety.

As shown in Scheme 1B, once the coordination mode is changed to O-binding, the final step of N_2O cleavage happens to complete the reaction to yield the final product **P$_O$**, for which a facile protonation occurs to yield the experimentally characterized neutral product complex.[8, 13]

As seen from Figure 1, this process's transition state **TS$_{NNO}$-Fe$_{b3}$** in the two-electron pathway is of lower energy than both the first step of NO coupling and the second step of binding mode switch, which is again stabilized via the coordination of O'N'N to the non-heme Fe(III) center.[6c, d] The overall NO-to-N_2O conversion process in the native NOR two-electron mechanism is thermodynamically very favorable with a reaction free energy of -37.4 kcal/mol.

Because BF_3 in the novel one-electron pathway cannot coordinate to O' to exert the similar stabilization effect of the non-heme site, this N-O bond breaking **TS$_{NNO}$** has a significantly high energy: 11.34 and 12.42 kcal/mol for Fe and Co respectively. As seen from Table 1, the N-O bond length continuously increases along the one-electron reaction pathway for both Fe and Co to prepare for its breakage, with the largest elongation occurring in this N_2O cleavage step: 0.2 Å (see Figure 2).

Similar to previous steps in this one-electron reaction pathway, the Fe system is still more favorable for N_2O cleavage. In **TS$_{NNO}$-Fe**, the N–O bond is 0.01 Å longer (See Figure 2) compared to **TS$_{NNO}$-Co**, making it a more ready for breaking and thus leading to a relatively lower barrier. This may originate from the easier oxidation of Fe to donate the electron to NO, which populates in the anti-bonding orbital to weaken it for easier cleavage.

As shown in Table S22, the M/O charges in the **P$_O$-Fe** and **P$_O$-Co** are 1.272/-0.848 e and 1.220/-0.763 e respectively, so the Fe–O bond has stronger coulombic attraction than the Co-O bond. As shown in Table 1 and Figure 1, **P$_O$-Fe** is much more stable than **P$_O$-Co**. **P$_O$-Fe** is also more favorable than **P$_O$-Fe$_{B3}$**, which is probably due to the shorter and stronger O–B bond (1.438 Å) and heme Fe–O bond (1.758 Å) compared to corresponding O–Fe$_B$ bond (1.749 Å) and Fe$_{b3}$–O bond (1.846 Å) in the two-electron

cis:b3 pathway.[6c, d] The longer bond lengths is associated with the fact that the LA non-heme Fe_B site is restrained by the protein environment to make it difficult to move too close for short/strong Fe-O-Fe bonding, while the LA BF_3 in the one-electron pathway is free to move to stabilize the O binding to heme Fe. Although the Fe porphyrin with BF_3 complex is highly effective in the initial NO reduction, its strong stability may hinder further steps in the catalytic cycle, particularly compared to the enzyme and Co system. In contrast, the Co system has a similar product energy to the enzyme's, suggesting that it may have the potential to be further developed for catalytic NO coupling.

Overall, as shown in Figure 1, the NO-to-N_2O reaction in both the novel one-electron pathways of heme models with LA and two-electron pathway in the native NOR system are kinetically and thermodynamically favorable to occur, as observed experimentally.

However, compared to the previously studied native NOR reaction with only the NO coupling step as the RDS, the novel one-electron pathways have different RDS features that depend on the metal center: 1) for Fe, instead of having one RDS of N–N coupling, the N_2O cleavage step has a similar barrier due to the non-ring structure here to stabilize the N_2O moiety; 2) for Co, the rate limiting step is the binding mode transition.

As seen from Figure 1, every species in the one-electron pathway after reactants is more favorable for Fe than Co. The overall RDS $\Delta G^{\ddagger}$ of 17.02 kcal/mol of the Co heme model is clearly higher than that of 11.44 kcal/mol for Fe, which is in good agreement with the experimentally observed higher N_2O yield from using the Fe heme vs. the Co porphyrin.[8, 13] Therefore, our computational results support the more favorable use of Fe in the heme center for the biological NOR function, which is the metal evolutionarily chosen for native bacNOR.[3]

Above results and discussion also show that with the same Fe heme center, the novel one-electron NO reduction pathway is kinetically competitive to the native two-electron process due to similar RDS barriers and thermodynamically much more favorable (see Figure 1). These features make them an interesting alternative route for NO reduction that is of broad general biological, environmental, and industrial importance.[1b, 3a, b, 4] This new one-electron pathway has been recently implemented for a biosynthetic NOR model with both heme/non-heme sites.[14a]

Conclusion

In summary, we have uncovered the complete mechanistic pathway information of the unprecedented NO-to-N_2O reaction that requires only one electron with Fe/Co heme and Lewis acid. The computational results confirmed that the Fe heme model, as the most abundant and widely used metalloporphyrin, is more reactive compared to Co, as found experimentally.[8, 13] Moreover, the quantum chemical investigation here for the first time, offer important geometric and electronic insights into the role of metal center on this novel NO coupling pathway. For instance, a metal center with a relatively lower reduction potential to donate an electron for NO reduction and N-O cleavage, and with a relatively larger size to facilitate the N/O coordination mode switch, is determined to be kinetically and thermodynamically more favorable. Results also offer the first evidence that this new one-electron NO reduction chemistry is kinetically competitive and thermodynamically more favorable than the native pathway, which builds an important mechanistic basis to support its use as a potential alternative for NO reduction. Therefore, it may initiate additional studies to further optimize this new chemistry with different metal centers, Lewis acids as well as other components of heme. Overall, these novel mechanistic results support to open a new venue of future development of related NO reduction agents in biology, environment, and industry.

Computational Details

All calculations were performed using Gaussian 16.[21] Full geometry optimizations, using unsubstituted porphine (Por) macrocycle, were conducted for all studied chemical species, using the PCM formalism[22] with CH_2Cl_2 solvent as used experimentally.[8, 13] Frequency calculations on the optimized structures were used to verify the nature of the corresponding stationary states on their potential energy surfaces and provide zero-point energy corrected electronic energies (E_{ZPE}'s), enthalpies (H's), and Gibbs free energies (G's) at the experimental reaction temperature 273.15 K, in addition to electronic energies. The used method includes the mPW1PW91[23] functional with the basis set of Wachters' basis[24] for iron, 6-311++G(2d,2p) for 1st shell atoms (atoms bonded to iron, and NO and BF_3), and 6-31G(d) for other atoms as used recently in reaction mechanistic studies of similar NO-containing systems.[8, 13, 18] The Intrinsic Reaction Coordinate (IRC) calculations in Gaussian 16 were used to further confirm the connection between each transition state and its preceding and subsequent species, besides the inspection of the imaginary vibrational mode of the transition state.

As the reaction mechanism may be affected by the conformations and spin states, these effects were examined first. The conformations of the species in the reaction pathway were built to be consistent with the metal bound hyponitrite intermediate structures from the previous computational study on the same systems.[8, 13] A systematic spin state investigation (see Supporting Information for details) was performed to determine the most favorable spin state for each species, which was used in the main text discussion.

Acknowledgements

This work was supported by an NIH grant GM085774 to YZ and an NSF grant CHE-2154603 to GBRA.

Keywords: nitrogen oxides • reaction mechanism • density functional calculations • iron • cobalt

[1] a) E. Culotta, D. E. Koshland, Jr., *Science* **1992**, *258*, 1862-1865; b) B. A. Averill, *Chem. Rev.* **1996**, *96*, 2951-2964; c) K. K. K. Chung, B. Thomas, X. J. Li, O. Pletnikova, J. C. Troncoso, L. Marsh, V. L. Dawson, T. M. Dawson, *Science* **2004**, *304*, 1328-1331; d) L. Cheng, G. B. Richter-Addo, in *The Porphyrin Handbook, Vol. 4* (Eds.: R. Guilard, K. M. Kadish, K. M. Smith), Academic Press, San Diego, **2000**, pp. 219-292; e) V. Ullrich, R. Kissner, *J. Inorg. Biochem.* **2006**, *100*, 2079-2086; f) S. Aono, *Chem. Soc. Rev.* **2008**, *24*, 3137-3146; g) W. Flores-Santana, C. Switzer, L. A. Ridnour, D. Basudhar, D. Mancardi, S. Donzelli, D. D.

Thomas, K. M. Miranda, J. M. Fukuto, D. A. Wink, *Arch. Pharm. Res.* **2009**, *32*, 1139-1153.

[2] J. MacMicking, Q.-W. Xie, C. Nathan, *Annu Rev Immunol.* **1997**, *15*, 323-350.

[3] a) C. Ferousi, S. H. Majer, I. M. DiMucci, K. M. Lancaster, *Chem. Rev.* **2020**, *120*, 5252−5307; b) A. J. Timmons, M. D. Symes, *Chem. Soc. Rev.* **2015**, *44*, 6708-6722; c) C. J. White, A. L. Speelman, C. Kupper, S. Demeshko, F. Meyer, J. P. Shanahan, E. E. Alp, M. Hu, J. Zhao, N. Lehnert, *J. Am. Chem. Soc.* **2018**, *140*, 2562−2574.

[4] a) X. Zhang, B. B. Ward, D. M. Sigman, *Chem. Rev.* **2020**, *120*, 5308−5351; b) L. Han, S. Cai, M. Gao, J.-y. Hasegawa, P. Wang, J. Zhang, L. Shi, D. Zhang, *Chem. Rev.* **2019**, *119*, 10916−10976.

[5] a) T. Tosha, Y. Shiro, *Iubmb Life* **2013**, *65*, 217-226; b) Y. Shiro, H. Sugimoto, T. Tosha, S. Nagano, T. Hino, *Phil. Trans. R. Soc. B* **2012**, *367*, 1195-1203.

[6] a) H. Kumita, K. Matsuura, T. Hino, S. Takahashi, H. Hori, Y. Fukumori, I. Morishima, Y. Shiro, *J. Biol. Chem.* **2004**, *279*, 55247-55254; b) L. M. Blomberg, M. R. A. Blomberg, P. E. M. Siegbahn, *Biochim. Biophys. Acta* **2006**, *1757*, 240-252; c) M. R. A. Blomberg, P. E. M. Siegbahn, *J Comput Chem* **2016**, *37*, 1810-1818; d) M. R. A. Blomberg, *Biochemistry* **2017**, *56*, 120-131; e) J. P. Collman, A. Dey, Y. Yang, R. A. Decreau, T. Ohta, E. I. Solomon, *J. Am. Chem. Soc.* **2008**, *130*, 16498-16499; f) S. Chakraborty, J. Reed, J. T. Sage, N. C. Branagan, I. D. Petrik, K. D. Miner, M. Y. Hu, J. Y. Zhao, E. E. Alp, Y. Lu, *Inorg. Chem.* **2015**, *54*, 9317-9329; g) Y.-W. Lin, N. Yeung, Y.-G. Gao, K. D. Miner, S. Tian, H. Robinson, Y. Lu, *Proc. Natl. Acad. Sci. USA* **2010**, *107*, 8581-8586; h) J. Wang, M. P. Schopfer, S. C. Pulu, A. A. N. Sarjeant, K. D. Karlin, *Inorg. Chem.* **2010**, *49*, 1404-1419; i) A. Bhagi-Damodaran, J. Reed, Q. Zhu, Y. Shi, P. Hosseinzadeh, B. A. Sandovall, K. A. Harden, S. Wang, M. R. Sponholtz, S. Dwaraknath, Y. Zhang, P. Moënne-Loccoz, Y. Lu, *Proc. Natl. Acad. Sci. U. S. A.* **2018**, *115*, 6195–6200; j) S. Chakraborty, J. Reed, M. Ross, M. J. Nilges, I. D. Petrik, S. Ghosh, S. Hammes-Schiffer, J. T. Sage, Y. Zhang, C. E. Schultz, Y. Lu, *Angew. Chem.-Int. Ed.* **2014**, *53*, 2417-2421.

[7] a) B. B. Wayland, L. W. Olson, *J. Am. Chem. Soc.* **1974**, *96*, 6037-6041; b) I. Lorkovic, P. C. Ford, *J. Am. Chem. Soc.* **2000**, *122*, 6516-6517.

[8] E. G. Abucayon, R. L. Khade, D. R. Powell, Y. Zhang, G. B. Richter-Addo, *J. Am. Chem. Soc.* **2018**, *140*, 4204-4207

[9] a) R. A. Baglia, M. Dürr, I. Ivanović-Burmazović, D. P. Goldberg, *Inorg. Chem.* **2014**, *53*, 5893-5895; b) R. A. Baglia, C. M. Krest, T. Yang, P. Leeladee, D. P. Goldberg, *Inorg. Chem.* **2016**, *55*, 10800-10809; c) P. Leeladee, R. A. Baglia, K. A. Prokop, R. Latifi, S. P. de Visser, D. P. Goldberg, *J. Am. Chem. Soc.* **2012**, *134*, 10397-10400.

[10] a) S. Bang, Y.-M. Lee, S. Hong, K.-B. Cho, Y. Nishida, M. S. Seo, R. Sarangi, S. Fukuzumi, W. Nam, *Nat. Chem.* **2014**, *6*, 934-940; b) S. Fukuzumi, K. Ohkubo, Y.-M. Lee, W. Nam, *Chem. Eur. J.* **2015**, *21*, 17548-17559; c) T. Devi, Y.-M. Lee, W. Nam, S. Fukuzumi, *Coord. Chem. Rev.* **2020**, *410*, 213219.

[11] a) M. P. Doyle, *Chem. Rev.* **1986**, *86*, 919-939; b) M. P. Doyle, R. R. Duffy, M., L. Zhou, *Chem. Rev.* **2010**, *110*, 704-724.

[12] a) D. Lionetti, S. Suseno, E. Y. Tsui, L. Lu, T. A. Stich, K. M. Carsch, R. J. Nielsen, W. A. Goddard, III, R. D. Britt, T. Agapie, *Inorg. Chem.* **2019**, *58*, 2336-2345; b) Y. Liu, T.-C. Lau, *J. Am. Chem. Soc.* **2019**, *141*, 3755-3766; c) G. Chen, L. Ma, P.-K. Lo, C.-K. Mak, K.-C. Lau, T.-C. Lau, *Chem. Sci.* **2021**, *12*, 632-638; d) A. Corma, H. García, *Chem. Rev.* **2002**, *102*, 3837-3892; e) L. Dong, Y. Wang, Y. Lv, Z. Chen, F. Mei, H. Xiong, G. Yin, *Inorg. Chem.* **2013**, *52*, 5418-5427; f) I. Garcia-Bosch, R. E. Cowley, D. E. Díaz, R. L. Peterson, E. I. Solomon, K. D. Karlin, *J. Am. Chem. Soc.* **2017**, *139*, 3186-3195.

[13] E. G. Abucayon, R. L. Khade, D. R. Powell, Y. Zhang, G. B. Richter-Addo, *Angew. Chem. Int. Ed.* **2019**, *58*, 18598 – 18603.

[14] a) S. Sabuncu, J. H. Reed, Y. Lu, P. Moenne-Loccoz, *J. Am. Chem. Soc.* **2018**, *140*, 17389−17393; b) M. Jana, C. J. White, N. Pal, S. Demeshko, C. Cordes, F. Meyer, N. Lehnert, A. Majumdar, *J. Am. Chem. Soc.* **2020**, *142*, 6600-6616; c) N. Pal, C. J. White, S. Demeshko, F. Meyer, N. Lehnert, A. Majumdar, *Inorg. Chem.* **2021**, *60*, 15890-15900; d) P. Ghosh, M. Stauffer, V. Hosseininasab, S. Kundu, J. A. Bertke, T. R. Cundari, T. H. Warren, *J. Am. Chem. Soc.* **2022**, *144*, 15093-15099; e) A. Dey, J. B. Gordon, T. Albert, S. Sabuncu, M. A. Siegler, S. N. MacMillan, K. M. Lancaster, P. Moënne-Loccoz, D. P. Goldberg, *Angew. Chem. Int. Ed.* **2021**, *60*, 21558-21564; f) J. Lu, B. Bi, W. Lai, H. Chen, *Angew. Chem. Int. Ed.* **2019**, *58*, 3795-3799.

[15] Y. Wei, A. Tinoco, V. Steck, R. Fasan, Y. Zhang, *J. Am. Chem. Soc.* **2018**, *140*, 1649-1662

[16] a) A. Bhagi-Damodaran, M. A. Michael, Q. H. Zhu, J. Reed, B. A. Sandoval, P. Moënne-Loccoz, Y. Zhang, Y. Lu, *Nat. Chem.* **2017**, *9*, 257-263; b) J. H. Reed, Y. Shi, Q. Zhu, S. Chakraborty, E. N. Mirts, I. D. Petrik, A. Bhagi-Damodaran, M. Ross, P. Moënne-Loccoz, Y. Zhang, Y. Lu, *J. Am. Chem. Soc.* **2017**, *139*, 12209-12218.

[17] a) M. R. A. Blomberg, *Inorg. Chem.* **2020**, *59*, 11542-11553; b) M. R. A. Blomberg, *Chem. Soc. Rev.* **2020**, *49*, 7301-7330.

[18] a) E. G. Abucayon, R. L. Khade, D. R. Powell, M. J. Shaw, Y. Zhang, G. B. Richter-Addo, *Dalton Trans.* **2016**, *45*, 18259-18266; b) E. G. Abucayon, R. L. Khade, D. R. Powell, Y. Zhang, G. B. Richter-Addo, *J. Am. Chem. Soc.* **2016**, *138*, 104-107.

[19] D. R. Lide, *CRC Handbook of chemistry and physics*, 87th ed., Taylor & Francis, Boca Raton, **2006**.

[20] D. Dolphin, R. H. Felton, *Acc. Chem. Res.* **1974**, *7*, 26-32.

[21] M. J. Frisch, G. W. Trucks, H. B. Schlegel, G. E. Scuseria, M. A. Robb, J. R. Cheeseman, G. Scalmani, V. Barone, G. A. Petersson, H. Nakatsuji, X. Li, M. Caricato, A. V. Marenich, J. Bloino, B. G. Janesko, R. Gomperts, B. Mennucci, H. P. Hratchian, J. V. Ortiz, A. F. Izmaylov, J. L. Sonnenberg, D. Williams-Young, F. Ding, F. Lipparini, F. Egidi, J. Goings, B. Peng, A. Petrone, T. Henderson, D. Ranasinghe, V. G. Zakrzewski, J. Gao, N. Rega, G. Zheng, W. Liang, M. Hada, M. Ehara, K. Toyota, R. Fukuda, J. Hasegawa, M. Ishida, T. Nakajima, Y. Honda, O. Kitao, H. Nakai, T. Vreven, K. Throssell, J. A. Montgomery, Jr., J. E. Peralta, F. Ogliaro, M. J. Bearpark, J. J. Heyd, E. N. Brothers, K. N. Kudin, V. N. Staroverov, T. A. Keith, R. Kobayashi, J. Normand, K. Raghavachari, A. P. Rendell, J. C. Burant, S. S. Iyengar, J. Tomasi, M. Cossi, J. M. Millam, M. Klene, C. Adamo, R. Cammi, J. W. Ochterski, R. L. Martin, K. Morokuma, O. Farkas, J. B. Foresman, D. J. Fox, Gaussian 16, Revision C.01. ed., Gaussian, Inc., Wallingford CT, **2019**.

[22] a) M. Cossi, V. Barone, R. Cammi, J. Tomasi, *Chem. Phys. Lett.* **1996**, *255*, 327-335; b) M. Cossi, V. Barone, B. Mennucci, J. Tomasi, *Chem. Phys. Lett.* **1998**, *286*, 253-260; c) M. Cossi, G. Scalmani, N. Rega, V. Barone, *J. Chem. Phys.* **2002**, *117*, 43-54; d) B. Mennucci, J. Tomasi, *J. Chem. Phys.* **1997**, *106*, 5151-5158.

[23] C. Adamo, V. Barone, *J. Chem. Phys.* **1998**, *108*, 664-675.

[24] A. J. Wachters, *J. Chem. Phys.* **1970**, *52*, 1033-1036.

Entry for the Table of Contents

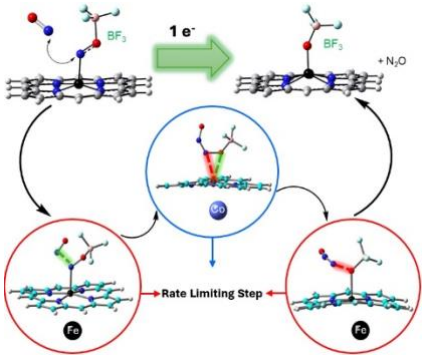

Compared to native nitric oxide reductases using a two-electron process, Fe and Co hemes, activated by BF_3, were recently found to effect this reaction with one electron. Our mechanistic study revealed their complete reaction pathways and advantageous reactivity origins of Fe heme compared to Co and the native pathway.